

# Kinetics of the Hopcalite-Catalyzed Oxidation of Carbon Monoxide

MICHAEL I. BRITTAN, HARDING BLISS, and CHARLES A. WALKER

Yale University, New Haven, Connecticut

The oxidation of carbon monoxide with Hopcalite catalyst was studied in an isothermal recycling reactor with special attention paid to the changes of gas phase compositions with time.

Conversion-time data exhibit significant departures from first-order behavior often ascribed to this reaction. In early stages the reaction rate declines more rapidly than would a first-order reaction; later the reverse is true. A mechanism, based on careful analyses of the literature and of our observations, is proposed. A kinetic model based on this mechanism is shown to reproduce the data of any run satisfactorily, but there is a considerable variation in values of the constants from run to run.

The catalytic oxidation of carbon monoxide near ambient temperature is the subject of this study. The reaction is an interesting and challenging one because, when oxide catalysts are used, interactions between gas and solid phases beyond simple catalysis are often involved. The reaction is of practical interest, as well, since carbon monoxide is a common pollutant.

The catalyst used was commercial Hopcalite (a mixture of oxides of manganese and copper and small quantities of other oxides).

This reaction has been the subject of much previous work, but its complexity and certain special circumstances, for example, the large heat of reaction (67.6 kcal./g. mole carbon monoxide) have led to considerable disagreement. The basic objectives of the present work were to carry out experiments with careful regard to these complexities and to establish, if possible, a mechanism and kinetic model to explain the results.

The reaction was carried out in a batch recirculation differential reactor. The range of variables was as follows:

Temperature:	40°C. (majority of runs), 28°C., 50°C.
Initial carbon monoxide:	26 to 108 mm. Hg.
Initial oxygen:	0 to 376 m. Hg.
Initial carbon dioxide:	2* to 84 mm. Hg.
Total pressure:	800 to 833 mm. Hg. This was attained with diluent nitrogen
Catalyst weight:	About 3 g.
Reactor gas volume:	3,194 cc.

\* Since initial time was taken at a point somewhat after initial contact with the catalyst, some product carbon dioxide was always present. See section Operating Pressure.

## SUGGESTIONS FROM THE LITERATURE

A comprehensive survey of the extensive literature on this reaction is presented by Brittan (7). Those references bearing on the aims and methods of the experimentation will be touched on briefly here; those having to do with kinetics and mechanism will be deferred to appropriate later sections.

### Experimental Problems

Shortcomings in experimental techniques are probably responsible for some of the discrepancies in the literature. For instance, the activity and behavior of the catalysts are

critically influenced by their preparation, their history, and even their environment between runs. This has received little attention.

Although the heat of reaction is large, measurements of the catalyst temperature during reaction are generally absent; large temperature rises have been reported in some investigations (1, 24, 25, 39, 41, 47, 57). With such a large heat effect, it is unlikely that isothermal conditions were attained in much of the previous work.

The possible presence of fluid-film and catalyst pore concentration and temperature gradients was rarely explored. These can exhibit great rate influencing effects, particularly in the often used static experiments.

A notable shortcoming in many investigations is the dependence on total pressure measurements for determination of reaction extent in batch experiments. There is ample evidence in the literature (see below) that the oxide catalysts undergo reaction in addition to acting as catalysts; thus, the reaction cannot be described so simply as  $\text{CO} + 1/2 \text{O}_2 = \text{CO}_2$ , and total pressure measurements are insufficient. Analyses of the gas compositions in a region of known pressure and constant temperature are essential to clarify this matter.

For these reasons, this experimentation was designed to:

1. Specify as completely as possible the nature, history, and storage of the catalyst
2. operate under such conditions that the reaction was isothermal
3. minimize diffusional effects
4. permit measurements of gas compositions at known pressure and constant temperature so that the true course of the reaction could be followed. To this end, the whole reactor (not merely the catalyst) was held at constant temperature.

### Consensus of Findings

Notwithstanding differences and inconsistencies in much of the previous work, there is general agreement on many points. The catalytic oxides are almost invariably nonstoichiometric in composition (36, 48, 59, 69, 70, and others). The catalyst activity appears to be dependent on the amount of available oxygen in the oxide (1, 9 to 12, 21, 38, 39, 43, 47, 52, 53, 61, 62, 65). Reduction of the oxide causes a lowering of its activity, and the data of some workers (11, 39) suggest a linear relationship between the amount of oxygen removed and the decline in activity. Several workers have reported that the activity of fresh catalysts is high but declines with use (11, 12, 42, 47, 65). The activity is apparently also permanently impaired by

Michael I. Brittan is with the Anglo American Corporation of South Africa, Limited, Crown Mines, Johannesburg, South Africa.

severe reductions of the oxide (1, 47). Adsorption of moisture poisons the oxides at ordinary temperatures (1, 11, 19, 22, 40, 42, 47, 53, 62, 67, 69, 70), but the moisture can be expelled at moderate temperatures.

A feature of the reaction noted in a large number of studies is the direct participation of the catalyst in the reaction. Higher oxides such as Hopcalite are readily reduced by carbon monoxide forming gaseous carbon dioxide. The reduced oxide can be reoxidized by contact with oxygen though this reaction appears to be slow and incomplete at ordinary temperatures (1, 27, 37, 47, 49, 57, 58, 74).

The fact that these catalysts are nonstoichiometric and may participate directly in the reaction makes it imperative that the gas compositions be followed so that the extent of this participation may be found. Poisoning by water must be avoided.

## EXPERIMENTAL

The reaction was conducted by charging mixtures of carbon monoxide, oxygen, and nitrogen (and, on occasion, carbon dioxide) to a closed-loop reactor and circulating them continuously through a short bed of Hopcalite catalyst. The entire reactor was immersed in a constant temperature bath. Gas samples were withdrawn from the reactor at suitable time intervals for analysis to monitor the progress of reaction. Runs were usually continued to virtually 100% conversion.

The reactor of Long (44), modified for this work, was constructed of glass piping (Figure 1) and had a total volume of  $3,194 \pm 5$  cc. The assembly consists of a horizontal section of 4-in. pipe in which the blower is mounted in an annular Teflon insert, a loop of 1-in. diameter pipe connecting the ends of the blower section and containing the catalyst (a bed about  $\frac{3}{8}$  in. in depth and supported on stainless steel wire mesh grid) and a sampling port sealed with chromatograph septums, a manifold of copper tubing with provisions for adding and removing gases and for measurement of pressure, and a water bath with temperature control to  $\pm 0.05^\circ\text{C}$ . Thermocouples are located in the catalyst bed, in the gas downstream from the blower and in the water bath.

The chromatographic analyses of the gases used in this work are as follows:

	Percentage of			
	CO	O <sub>2</sub>	N <sub>2</sub>	CO <sub>2</sub>
Carbon monoxide	99.90	0.02	0.08	
Oxygen		99.75	0.25	
Nitrogen			99.996	
Carbon dioxide		0.03	0.12	99.85

Since complete dryness of all gases was necessary, they (except carbon dioxide) were passed through tubes packed with Linde 5A molecular sieves. Since carbon dioxide is strongly retained by molecular sieves at ambient temperatures silica gel was used as the desiccant in this case. The gas feed lines formed a manifold system connected to the reactor as shown in Figure 1 enabling any of the five gases to be tapped as required.

## Gas Analysis System

A chromatographic technique was devised for all four gaseous components using a Beckman GC-2 Chromatograph with both a silica gel and a 5A molecular sieve column in conjunction with a dual-column valve. The details of the technique are given elsewhere (7). The precision of the analysis was estimated to be within  $\pm 0.2\%$ .

Gas samples were withdrawn from the reactor with 5 cc. hypodermic syringes equipped with  $1\frac{1}{2}$  in. Huber point needles which prevented plugging of the needle on penetration of the septums. Since a complete analysis of all components was obtained, it was not necessary to know or duplicate accurately the sample volume. The sample volume withdrawn from the reactor was about 3 cc. and was purged until 2 cc. remained immediately preceding injection into the chromatograph. On average, about 1% of the gas in the reactor was lost to the samples in the course of a run. The nitrogen diluent constituted the major proportion of the gas and thus the amounts of

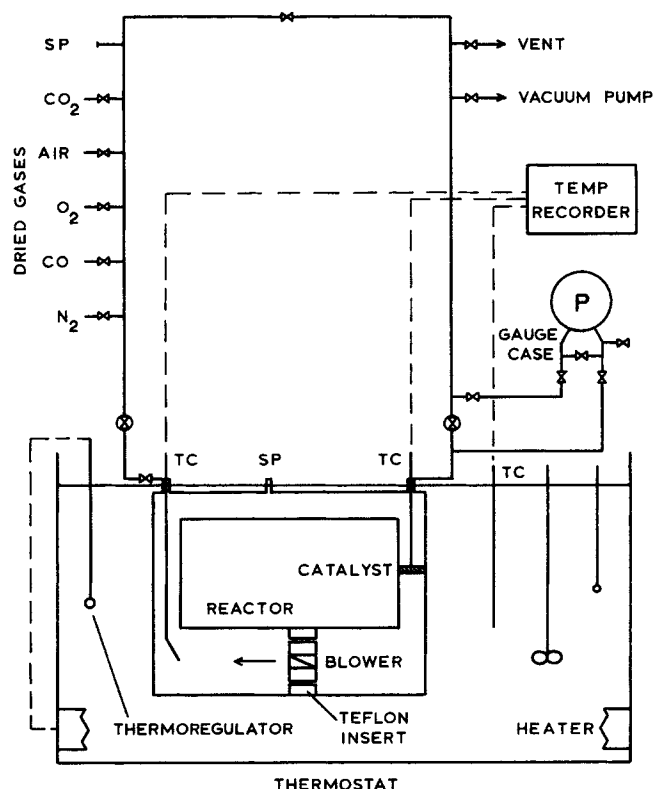


Fig. 1. Reactor and support system.

reaction components removed were insignificant.

At high reaction rates, the frequency of the gas sampling was greater than the maximum frequency with which they could be analyzed imposed by the 7 min. analysis time. Thorough sealing of the syringes permitted the storage of these samples in the syringes prior to injection into the chromatograph.

## Catalyst

The Hopcalite used was the same as that employed in Mine Safety Appliances M-S-A All-Service Gas Mask Canisters. This was stored in a dry atmosphere prior to use. The catalyst used in A-series runs consisted of 3.05 g. of Hopcalite taken directly from storage. That used in B-series runs was pretreated by heating in vacuo at  $185^\circ\text{C}$ . for 3 hr. The bed of B catalyst weighed 2.988 g.

Analysis of the catalyst for metal components (60) indicated manganese as the major component, copper as the minor, very small amounts of cobalt and silver, and traces of aluminum, iron, nickel, magnesium, and barium. A recently reported analysis of Hopcalite from the same source is 78.3% manganese dioxide, 13.1% cupric oxide, traces of other elements, 7.9% loss on ignition (15). The fresh catalyst was analyzed volumetrically for available oxygen content by methods described in such textbooks as that of Kolthoff and Sandell. The result (13.30% available oxygen) is in the range of values reported in the literature (1, 39).

The catalyst consisted of black granules of irregular shape which can be characterized as to size by noting that the equivalent sphere diameter would be 0.20 to 0.25 cm. Data on nitrogen adsorption and desorption at liquid nitrogen temperatures indicated the BET surface area to be about 300 sq.m./g. The method of Barrett, Joyner, and Halenda (3) was used to analyze the isotherm data and indicated an average micropore radius of approximately 30Å.

## Operating Procedure

With the thermostat at the required temperature, the reactor was evacuated, then charged with nitrogen and oxygen (in the great majority of runs) in the desired proportions but in quantities somewhat in excess of those required for the run. A ball valve at the reactor inlet was used to meter the gases to provide the required partial pressures as indicated by the pressure gauge. The blower was then switched on and the system left

to run in this way until steady state temperatures were approached. The contents of the reactor were bled until the total pressure at the steady state gas temperature was roughly midway between the initial pressure and the predicted final pressure of the run. This insured that the gas temperature would be approximately at the required level for the run. In the meantime, a syringe was inserted into the sample port in readiness for the first sample.

When both the gas and catalyst temperatures were approximately at steady state, the reactor was rapidly purged with the aid of the vacuum pump until the requisite partial pressures of nitrogen and oxygen remained. The necessary amount of carbon monoxide was immediately added and the shut-off valve at the reactor inlet closed. Several seconds were allowed for complete mixing of the gas, during which time the syringe was repeatedly flushed. On withdrawal of the needle, a stopwatch was started (thus marking  $t = 0$ ), the pressure read and the gas and catalyst temperature readings recorded. The sample was stored in the manner described earlier prior to injection into the chromatograph.

Shortly before extraction of the second sample a syringe was inserted into the sample port and flushed as before. When the sample was taken, the stopwatch was stopped and a second stopwatch started simultaneously. The elapsed time was recorded along with the pressure and temperature readings. This procedure was repeated until the run was terminated. Samples were taken after suitable composition changes rather than at definite time intervals. The samples were analyzed concurrently with the run.

TABLE 1. RUN CONDITIONS

Run No.	Initial partial pressures, mm. Hg.			Catalyst temp., °C.	Days elapsed between runs
	CO	O <sub>2</sub>	CO <sub>2</sub>		
A1	80	158	6	40	—
A2	81	159	4	40	2
A3	82	159	4	40	2
A4	79	159	4	40	2
A5	78	160	84	40	2
A6	79	376	5	40	2
A7	78	41	5	40	3
A8	83	161	2	40	0
A9	81	159	4	40	4
A10†	29	3	2	40	6
A11*	78	161	4	40	3
A12	104	99	4	40	5
A13	108	117	3	40	7
B1	82	103	24	40	—
B2	102	108	9	40	0
B3	102	108	8	40	1
B4	106	108	6	40	0
B5	102	109	7	40	2
B6	102	109	9	40	5
B7	108	109	5	40	0
B8	105	110	5	40	1
B9	106	109	6	40	1
B10	106	110	5	40	1
B11	99	110	7	40	10
B12	26	168	3	50	1
B13	27	0	2	40	1
B14	29	166	2	40	0
B15	28	168	2	40	1
B16	28	167	2	28	1
B17	29	168	3	40	1
B18	29	168	2	50	1
B19	28	168	2	40	1
B20	104	156	4	40	2
B21	105	157	3	40	1
B22	106	157	4	40	1

\* CO<sub>2</sub> added during run.

† O<sub>2</sub> added during run.

TABLE 2. SAMPLE DATA, RUN B22

Time, min.	Catalyst temp., °C.	Partial pressures, mm. Hg.		
		CO	O <sub>2</sub>	CO <sub>2</sub>
0.00	40.88	105.9	157.0	3.5
1.65	40.15	99.6	154.8	9.9
4.77	39.93	91.4	150.4	17.8
10.37	39.78	81.0	145.6	27.6
19.25	39.73	68.1	139.7	40.1
32.48	39.71	54.0	132.0	54.1
50.90	39.71	39.4	124.4	68.3
70.97	39.69	28.1	118.6	79.4
90.98	39.69	19.6	113.9	88.3
116.17	39.67	11.8	109.8	95.0
142.78	39.67	6.5	107.3	100.1
168.27	39.64	3.0	105.3	103.1
190.18	39.64	1.3	104.2	105.0

The reactor was evacuated after each run, and then (usually) filled with air slightly above atmospheric pressure.

## EXPERIMENTAL DATA

Experimental run conditions are shown in Table 1. The ranges of partial pressures studied are considerably larger than those of nearly all previous investigations. Total pressure was made up to 800 to 833 mm. Hg. with nitrogen so that gas samples would not be contaminated with air leakage into the syringe.

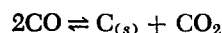
The partial pressure-time data for the thirty-five runs considered in the study are listed by Brittan (7). Data of a sample run are given in Table 2, and some are plotted in Figures 2 to 6. It may be noted in Table 2 that, after a slight catalyst temperature rise on admission of carbon monoxide when the reaction rate is highest, the catalyst temperature remained essentially constant during the run.

## ABSENCE OF EXTRANEEOUS RATE INFLUENCING EFFECTS

### Extraneous Catalytic Effects

A blank run without catalyst exhibited no reaction indicating the reactor and blower to be noncatalytic.

There was no evidence for the potentially competitive metal catalyzed reaction



often observable above 300°C. (2, 16, 32, 71). It is thermodynamically favorable below 900°C.

### Diffusional Effects

The possibility that resistance to exterior-film mass transfer influenced the reaction rate was tested by comparison of the rates of reaction at different gas velocities through the catalyst bed. Runs A1, A2, and A3 (see Figure 2) were carried out at one gas velocity and they exhibited an activity which was reasonably constant. Run A4 was conducted at a much lower gas velocity, and its position indicates only a small, if not negligible, difference. It is thus probable that exterior gas-film diffusion does not limit the reaction rate. Calculations made according to the method of Yoshida, Ramaswami, and Hougen (73) showed that even at the highest reaction rates, both external mass and heat transfer effects were of negligible importance. It may be added that the marked change in reaction rate with conversion is hardly consistent with diffusion as the controlling mechanism in the reaction.

A check on the possible presence of intraparticle concentration and temperature gradients was made using the criterion of Weisz and Hicks (68). This indicated that

operation was in a region where the catalyst effectiveness factor was unity even with the highest reaction rates encountered. In these calculations Knudsen diffusivity for a micropore radius of 30 Å. and a thermal conductivity of  $10^{-4}$  cal./ (cm.) (°C.) (sec.) (68) were used. A more desirable procedure would have been to reduce the particle size and determine the effect on the reaction rates. However, this was essentially impossible since the catalyst powdered easily and pressure drop complications would have been incurred with the smaller granules.

### GENERAL OBSERVATIONS ON THE SYSTEM

A significant feature of the system which has been noted by previous workers was the ready ability of the Hopcalite to convert carbon monoxide to carbon dioxide at the expense of some of its oxygen content. This is illustrated by run B13 (Figure 5 and Table 1). Reduced catalyst could be reoxidized by gaseous oxygen but, as with former investigations (1, 27, 37, 47, 57, 58, 74), oxygen uptake was apparently more sluggish than catalyst reduction by carbon monoxide.

The reaction rate was found to be strongly dependent on the partial pressure of carbon monoxide, weakly dependent on the oxygen partial pressure, and independent of the carbon dioxide partial pressure. This independence of carbon dioxide is illustrated by run A11 (Figure 3) and is confirmed in other investigations (1, 22, 23, 41, 69, 70). It should be noted, however, that the introduction of carbon dioxide before a run reduces the rate of that run as A5 (Figure 2) shows. This is probably due to adsorption of carbon dioxide on a catalyst surface oxygen (28, 30, 33, 34, 64 to 66). Such introduction of carbon dioxide before

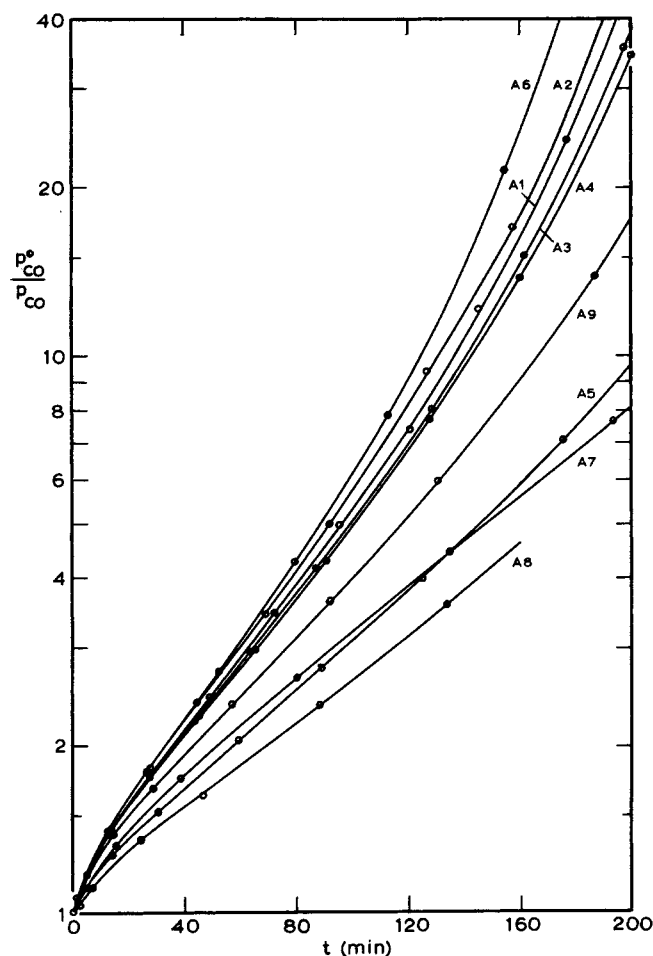


Fig. 2. First-order plot of carbon monoxide data, runs A1 to A9.

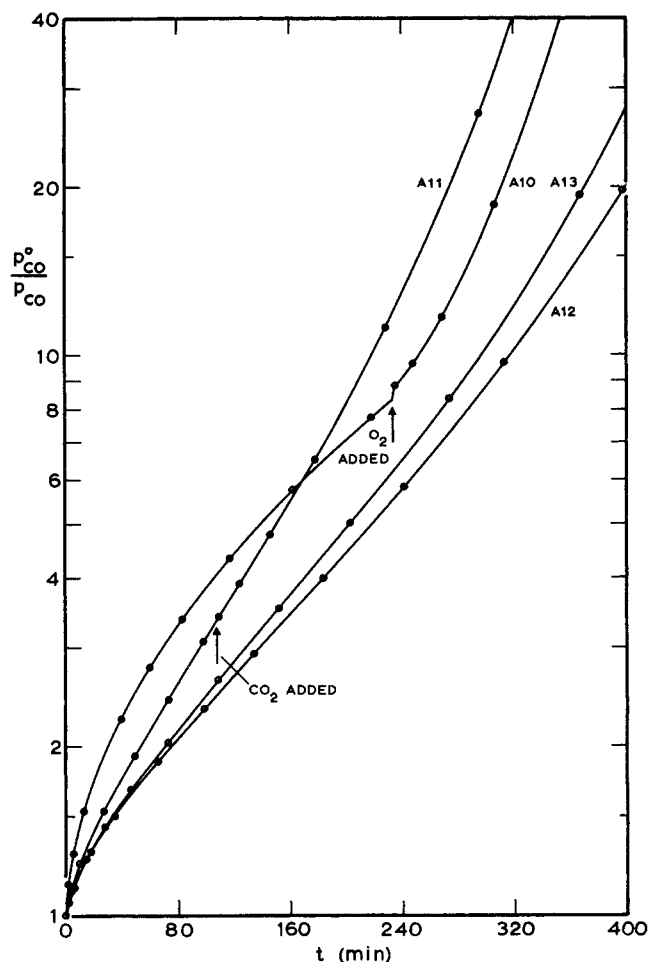


Fig. 3. First-order plot of carbon monoxide data, runs A10 to A13.

a run offers some competition with carbon monoxide for the sites, but it seems to be unable to do this once the sites are largely occupied.

Since the rate was primarily dependent on carbon monoxide partial pressure (1, 12, 14, 21, 23, 39, 41, 61, 63, 65) the reaction was provisionally taken to be first-order in that component:

$$-\frac{dp_{co}}{dt} = Kp_{co} \quad (1)$$

and plotted according to the integrated form

$$\ln \frac{p_{co}^0}{p_{co}} = Kt \quad (2)$$

The plots for most of the runs are thus shown in Figures 2 to 6. The run conditions relevant to Figures 2 to 6 are given in Table 1.

The activity of fresh catalysts was high but declined in the course of experimentation. This is exemplified in Figure 4 by the decline in slope of the first-order curves in passing from run B1 to B11. Similar observations have been made in previous investigations with manganese oxides and Hopcalite (11, 12, 42, 47, 65) and also with other oxides. The decrease in catalyst activity was found to be accelerated by reducing gas-phase conditions (relatively low oxygen:carbon monoxide) and minimized by oxidizing gas mixtures (relatively high oxygen:carbon monoxide) corresponding with the degree of oxidation of the catalyst. It was possible to attain reasonable plateaus of activity (or even on occasion to enhance the activity) by ensuring that oxidizing gas-phase conditions prevailed, thereby preventing appreciable reduction of (or actually

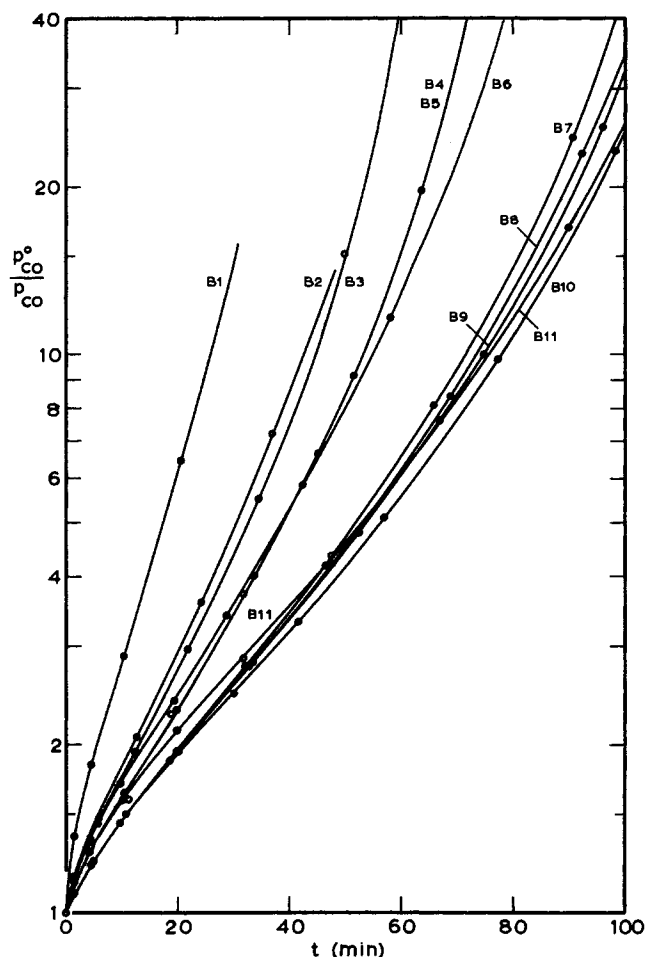


Fig. 4. First-order plot of carbon monoxide data, runs B1 to B11.

oxidizing) the catalyst. Thus, for example, run A6 (higher oxygen:carbon monoxide) is of higher activity than runs A1 to A4 (lower oxygen:carbon monoxide) and the activity of run A9 is greater than that of A7 (low oxygen:carbon monoxide). Run A8 cannot be used in this comparison because it was made almost immediately after A7 and the catalyst had not had time to recover from the low oxygen conditions of run A7.

Conditions between runs were also found to influence the catalyst activity. The decline in activity could be minimized by contacting the catalyst with oxygen for a sufficient period of time before a run. Thus, referring to Figure 4, for example, the marked activity decrease between runs B1 and B2 and between B6 and B7 is a result of their close proximity in time; each pair of runs was conducted on the same day. On the other hand, the runs of comparable activity (that is, B2 and B3, B4 to B6 and B7 to B11) were spaced one or more days apart thus allowing the catalyst time to reoxidize and recover some activity. Two runs in quick succession, however, impair permanently the activity, and thus B4 did not reattain the activity of B1.

When catalyst activity changes so much between runs, one cannot deny with certainty the possibility of such activity change during a run. This is felt to be improbable, however, because of the similar shapes of the first-order plots of all comparable runs. It is unlikely that activity changes within a run would have occurred in the same way.

The dependence of the catalyst activity on its degree of reduction or oxidation is in full accord with the results of earlier investigators (1, 9 to 12, 21, 38, 39, 43, 47, 52, 53, 61, 62, 65) who have associated the activity of the

catalyst with the quantity of its available oxygen.

It is apparent that the curves of Figures 2 to 6 are not linear and thus the reaction is not simple first-order in the partial pressure of carbon monoxide. The increased accuracy and completeness of the data of this work highlighted their definite cubic shape. Curvature similar to that to the left of the inflection points is evident from the first-order plots of some previous investigators (17, 45, 50). However, this trend in the data was disregarded by these investigators and the reaction assumed to be first-order. It may be noted that data obeying Elovich kinetics (see below) reported in some earlier studies (5, 6, 17, 21, 23, 50, 55, 56) if plotted according to Equation (2), would display the same curvature at low conversions. Such simple kinetic expressions are, however, inadequate to characterize the apparent complexities of the reaction. Neither a first-order expression nor the Elovich equation is commensurate with the cubic shape of the first-order curves of Figures 2 to 6. Furthermore, they do not adequately reflect the ramifications of such phenomena as the reduction and oxidation of the oxide catalyst.

## MECHANISM

### Previous Work

The literature survey revealed close similarity in the behavior of Hopcalite and manganese dioxide and some similarity between the behavior of Hopcalite and other oxides such as those of copper and nickel. In this discussion,

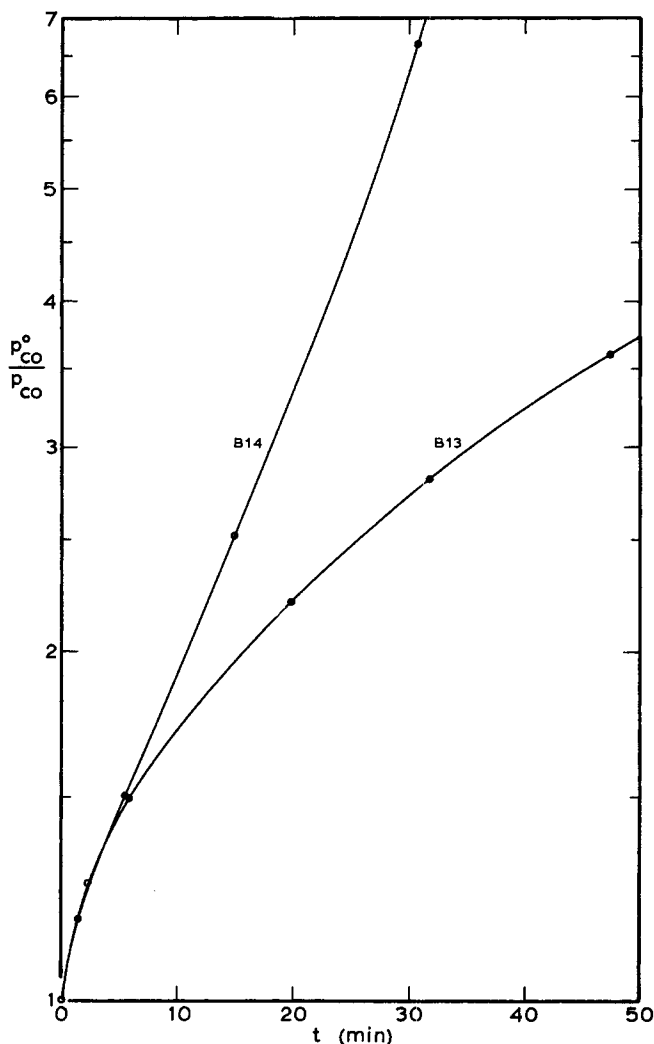
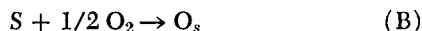
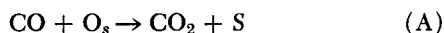


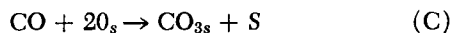
Fig. 5. First-order plot of carbon monoxide data, runs B13 and B14.

a distinction among these materials is not considered necessary.

The most fundamental mechanism postulated in the literature for Hopcalite and manganese oxide catalysts is the reduction-oxidation scheme originally proposed by Rogers, et al. (53) and subsequently cited by numerous investigators who often attributed it to Benton (4). This was formulated to describe the observations that carbon monoxide can be oxidized by the catalyst oxygen and that the reduced oxide is then able to take up oxygen. Representing the catalyst surface oxygen as  $O_s$  and a vacant site as  $S$ , the mechanism may be written



Garner and Ward (28, 30, 66) presumed that this basic mechanism was correct but concluded that reaction proceeds also by an intermediate carbonate ion:



The reversibility of reaction (D) is in accord with the observation that the carbonate state could be attained by adsorption of carbon dioxide on the surface. This is supported by studies of exchange of oxygen between carbon dioxide and the oxide surface (33 to 36, 64, 65).

A shortcoming of the oxidation-reduction scheme arises from experimental observations that the rate of catalyst reduction by carbon monoxide is considerably more rapid than the rate of its reoxidation by oxygen. The fact that the rate of the overall reaction is virtually independent of the oxygen partial pressure suggests the presence of a reaction path additional to reduction and oxidation of the oxide.

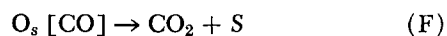
Roginskii and Zeldovich (54, 57, 58, 64) proposed a mechanism which avoids this shortcoming by assuming the adsorption of carbon monoxide to be the rate-controlling step; this is followed by reaction of the adsorbed carbon monoxide with both oxide and oxygen. Also postulated are reactions between adsorbed oxygen and carbon monoxide and reoxidation of the reduced oxide by gaseous oxygen. We believe this mechanism to be more promising than alternative schemes such as that of Bruns and Shurmovskaya (12).

#### A Proposed Mechanism

With  $O_s$  representing a catalyst surface oxygen site, the presumed primary and rate-controlling adsorption step can be written as follows:



Reduction of the catalyst to produce carbon dioxide can be represented as



where  $S$  is a vacant active site which can be regenerated as follows:

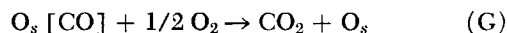


The experimental data provide evidence for reaction steps (E), (F), and (B). Qualitatively, one might expect reduction of the catalyst to occur when the carbon monoxide partial pressure is high at low conversions and oxidation of the catalyst to occur when the carbon monoxide partial pressure is low (provided sufficient oxygen is present). Participation of the oxide catalyst in the reaction would influence the stoichiometry of the gas phase. This would be reflected in the value of  $(2p_{O_2} - p_{CO})$ , a quan-

tity which should remain constant throughout a run if the reaction involves only gas-phase oxygen. However, the data when plotted indicate that the value of  $(2p_{O_2} - p_{CO})$  first rises, traverses a maximum and then declines. This is exactly in accord with expectations. At low conversions the oxide is being reduced and some catalyst oxygen is being used to convert the carbon monoxide. At high conversions, on the other hand, the catalyst is directly reoxidized by gaseous oxygen, the partial pressure of which thus falls at a greater rate than would otherwise occur.

Further substantiating evidence is provided by an examination of the cubic shape of the first-order curves of Figures 2 to 6. From Equation (2), the slope of these curves represents the first-order rate parameter,  $K$ , which according to reaction (E) is equal to  $kO_s$  where  $k$  is the rate constant for this reaction. The slope of the first-order curves (that is,  $kO_s$ ) first decreases, traverses a minimum at the inflection point and then increases. This can be interpreted as depletion of  $O_s$  in the early stages of reaction and reoxidation of the catalyst in later stages. The results of run B13 (Figure 5), which was conducted in the absence of gaseous oxygen, are also in accord with the postulated mechanism in that no point of inflection is observed.

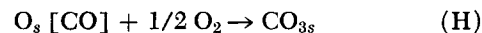
Reaction (F) must not be the only path by which carbon dioxide is formed, however, as an examination of run A10 (Figure 3) shows. In this run the small initial oxygen charge was reacted essentially to completion along with depletive reduction of the catalyst. When additional oxygen was admitted to the system there was a marked increase in carbon dioxide production. This strongly suggests a reaction between the added oxygen and the adsorbed carbon monoxide:



This reaction is the result of the elementary steps (29)



and we have written  $1/2 O_2$  in place of  $O_{Ads}$  as a convenience. Noting the evidence in the literature for an intermediate carbonate complex (8, 20, 28 to 30, 66, 72), it is likely that reaction (G) proceeds via this complex:



The carbonate complex then breaks down to carbon dioxide and a surface oxygen:



The reasons for indicating this reaction to be reversible have been stated previously. However, carbon dioxide has negligible effect on the overall rate (see Run A11), indicating that the equilibrium lies far to the right. With Reaction (D) written as irreversible, it will be seen that the sum of (D) and (H) is (G). It is thus not necessary to consider this complex as a separate species.

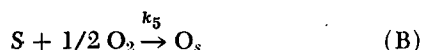
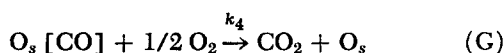
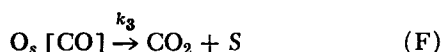
During this study it was observed that the amount of carbon dioxide produced was consistently slightly less than the amount of carbon monoxide consumed. This effect has also been reported by Bruns (11) and others (27, 37, 46, 49) and suggests that a small amount of carbon dioxide must be very firmly retained and released very slowly:



It is not likely that the desorption step is of importance in a kinetic analysis. Experimental observations indicated a very slow release of carbon dioxide into the gas phase

during periods between runs.

It is concluded that the significant reactions in a rate analysis are the following:



## A KINETIC MODEL

The major reactions of the mechanism with the rate constants given permit the formulation of a model. It is based on the assumption that the rate is controlled by the adsorption of carbon monoxide [reactions (E) and (K)] on  $\text{O}_s$  centers whose concentration is governed by the scheme as a whole. It must be observed that the fact that a model may fit kinetic data only lends support to the mechanism on which it is based; it does not prove the mechanism.

The rate-controlling step of carbon monoxide adsorption is taken as first-order in the partial pressure of carbon monoxide and proportional to the concentration of  $\text{O}_s$  adsorption sites:

$$-\frac{dp_{\text{CO}}}{dt} = (k_1 + k_2) \text{O}_s p_{\text{CO}} \quad (3)$$

With  $k = (k_1 + k_2)$

$$-\frac{dp_{\text{CO}}}{dt} = k \text{O}_s p_{\text{CO}} \quad (4)$$

Letting  $\theta$  denote the concentration of  $\text{O}_s [\text{CO}]$  and assuming that reaction order corresponds to molecularity

$$\frac{dp_{\text{CO}_2}}{dt} = (k_3 + k_4 p_{\text{O}_2}^{1/2}) \theta \quad (5)$$

$$-2 \frac{dp_{\text{O}_2}}{dt} = (k_4 \theta + k_5 \text{S}) p_{\text{O}_2}^{1/2} \quad (6)$$

Since (E) is a relatively slow reaction,  $\text{O}_s [\text{CO}]$  reacts to form carbon dioxide according to (F) and (G) as fast as it is formed. This conforms to the observation that the carbon dioxide produced is rapidly released to the gas phase and is substantiated by the experimental data which show that the partial pressure-time curve for carbon dioxide is virtually a mirror image of that for carbon monoxide (provided that the small quantity of carbon dioxide present at  $t = 0$  be accounted for). Consequently, a balance for  $\text{O}_s [\text{CO}]$  yields

$$k_1 \text{O}_s p_{\text{CO}} = (k_3 + k_4 p_{\text{O}_2}^{1/2}) \theta \quad (7)$$

It may be noted that this is tantamount to a quasistationary state assumption for  $\theta$ . Solving for  $\theta$ :

$$\theta = \frac{k_1 \text{O}_s p_{\text{CO}}}{k_3 + k_4 p_{\text{O}_2}^{1/2}} \quad (8)$$

Substituting for  $\theta$  in Equations (5) and (6) yields

$$\frac{dp_{\text{CO}_2}}{dt} = k_1 \text{O}_s p_{\text{CO}} \quad (9)$$

$$-2 \frac{dp_{\text{O}_2}}{dt} = \left\{ \frac{k_1 \text{O}_s p_{\text{CO}}}{k_3/k_4 + p_{\text{O}_2}^{1/2}} + k_5 \text{S} \right\} p_{\text{O}_2}^{1/2} \quad (10)$$

There remains only to eliminate the unknowns  $\text{O}_s$  and  $\text{S}$  from Equations (4), (9), and (10) in terms of observable quantities. From the reaction scheme

$$\begin{aligned} \frac{d\text{O}_s}{dt} &= -(k_1 + k_2) \text{O}_s p_{\text{CO}} + k_4 \theta p_{\text{O}_2}^{1/2} \\ &\quad + k_5 \text{S} p_{\text{O}_2}^{1/2} = \frac{dp_{\text{CO}}}{dt} - 2 \frac{dp_{\text{O}_2}}{dt} \quad (11) \end{aligned}$$

Integrating this equation, we get

$$\text{O}_s - \text{O}_s^0 = (p_{\text{CO}} - p_{\text{CO}}^0) - 2(p_{\text{O}_2} - p_{\text{O}_2}^0) \quad (12)$$

Let

$$c_1 = \text{O}_s^0 + 2p_{\text{O}_2}^0 - p_{\text{CO}}^0 \quad (13)$$

then

$$\text{O}_s = c_1 - (2p_{\text{O}_2} - p_{\text{CO}}) \quad (14)$$

Similarly, for  $\text{S}$

$$\frac{d\text{S}}{dt} = \frac{dp_{\text{CO}_2}}{dt} + 2 \frac{dp_{\text{O}_2}}{dt} \quad (15)$$

Integrating this equation, we get

$$\text{S} - \text{S}^0 = (p_{\text{CO}_2} - p_{\text{CO}_2}^0) + 2(p_{\text{O}_2} - p_{\text{O}_2}^0) \quad (16)$$

Let

$$c_2 = \text{S}^0 - 2p_{\text{O}_2}^0 - p_{\text{CO}_2}^0 \quad (17)$$

then

$$\text{S} = c_2 + (2p_{\text{O}_2} + p_{\text{CO}_2}) \quad (18)$$

It should be observed that  $\text{O}_s$  and  $\text{S}$  [Equations (12) and (16)] must have units of pressure. Substituting for  $\text{O}_s$  and  $\text{S}$  in (4), (9), and (10) yields the rate expressions for the three reaction components in final form:

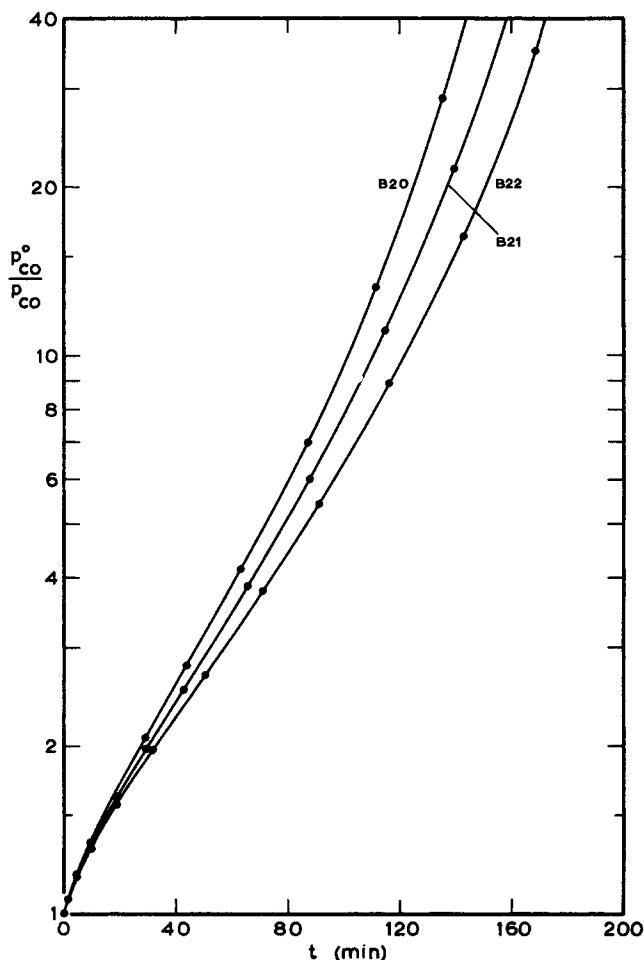


Fig. 6. First-order plot of carbon monoxide data, runs B20 to B22.

$$-\frac{dp_{CO}}{dt} = k [c_1 - (2p_{O_2} - p_{CO})] p_{CO} \quad (19)$$

$$\frac{dp_{CO_2}}{dt} = k_1 [c_1 - (2p_{O_2} - p_{CO})] p_{CO} \quad (20)$$

$$-2 \frac{dp_{O_2}}{dt} = \left\{ \frac{k_1 [c_1 - (2p_{O_2} - p_{CO})] p_{CO}}{k_3/k_4 + p_{O_2}^{1/2}} + k_5 [c_2 + (2p_{O_2} + p_{CO_2})] \right\} p_{O_2}^{1/2} \quad (21)$$

It may be noted that separate rate equations are required for each component since the reaction does not proceed stoichiometrically. The rate equations contain among them the six constants,  $k$ ,  $k_1$ ,  $k_3/k_4$ ,  $k_5$ ,  $c_1$ , and  $c_2$ .

#### Qualitative Behavior of the Model

It is interesting to examine the qualitative behavior of the above system of rate equations.

Equation (19), in the limiting case that  $(2p_{O_2} - p_{CO})$  remains constant, reduces to a straightforward first-order expression giving the kinetics most frequently reported in previous studies. As discussed earlier, however, the value of  $(2p_{O_2} - p_{CO})$  passes through a maximum in the course of a run. Consequently,  $[c_1 - (2p_{O_2} - p_{CO})]$  traverses a minimum, and this is in accordance with the cubic shape of the first-order curves of Figures 2 to 6.

Equation (20) indicates that the partial pressure-time curve for carbon dioxide is almost a mirror image of that for carbon monoxide in agreement with the experimental data. The difference between  $k$  and  $k_1$  accounts for the slight disparity between carbon monoxide consumption and carbon dioxide production.

In Equation (21) the factor  $(k_3/k_4 + p_{O_2}^{1/2})$  characterizes the competition between Reactions (G) and (F) determining whether  $O_s[CO]$  reacts with oxygen or breaks down into carbon dioxide and reduced catalyst. Higher oxygen partial pressures would, of course, assist the former reaction and thus decrease the degree of catalyst reduction. This is in accordance with the experimental results obtained with conditions of relatively high  $O_2 : CO$  as noted earlier.

Thus, the model behaves in the appropriate manner.

#### Reproduction of Data with the Model

The values of the constants of Equations (19) to (21) were determined by fitting the equations to the experimental partial pressure-time data. The procedure first involved the calculation of the reaction rates by numerical differentiation of the data. This provided values of the left-hand sides of Equations (19) to (21). Treating each equation individually, the method of least squares was then used to determine the constants. The details of the calculation are presented elsewhere (7).

The constants for run B6 were as follows (parenthetic figures are described below):

$$\begin{aligned} k &= 0.00737 \text{ (min.)}^{-1}(\text{mm. Hg.})^{-1} && (0.0114 \text{ to } 0.00261) \\ k_1 &= 0.00712 \text{ (min.)}^{-1}(\text{mm. Hg.})^{-1} && (0.0109 \text{ to } 0.00255) \\ O_s^0 &= 11.81 \text{ equiv. mm. Hg.} && (13.84 \text{ to } 4.09) \\ k_3/k_4 &= 3.13 \text{ (mm. Hg.)}^{1/2} && (18.66 \text{ to } 0.60) \\ k_5 &= 0.0085 \text{ (min.)}^{-1}(\text{mm. Hg.})^{-1} && (0.0155 \text{ to } 0.0025) \\ S^0 &= 0.95 \text{ equiv. mm. Hg.} && (5.16 \text{ to } 0.50) \end{aligned}$$

The capacity of the model with these constants to reproduce the data of run B6 is shown in Figure 7. The rate equations were integrated simultaneously with a Runge-Kutta technique with 2 min. time intervals.

Such reproduction of data was equally successful with

all runs tried (essentially all the B series and A12 and A13), but agreement in values of the constants among the runs was not good. The extreme ranges of each constant are indicated in parentheses. These discrepancies arise from errors due to small differences between large numbers inherent in factors such as  $[c_1 - (2p_{O_2} - p_{CO})]$  and also from differences in intrinsic catalyst activity. The use of average values of the constants of runs of similar activity was also found to yield good reproduction of the data.

#### DISCUSSION

Though different sets of constants are required for each run and each activity level, the good reproduction of the data by the kinetic model in all cases may be regarded as some endorsement of the model.

The constant  $k$  is always very little larger than  $k_1$  (the difference is  $k_2$ ). Thus the rate of adsorption of carbon monoxide must be greatly in excess of the rate of reaction of carbon monoxide to form strongly held carbon dioxide.

It was observed that runs exhibiting particularly low values of  $k$  also exhibit low values of average slopes in Figures 3, 4, and 6. This means, of course, that some of the discrepancies in values of the constants is real and not merely an inaccuracy in calculations. There must be some variation in intrinsic activity not accounted for in the model. Characterization of the activity decline was not practical because the decline was dependent on the conditions between runs. In the model an attempt was made to account for changes in activity during a run due to reduction (and partial reoxidation) of the catalyst oxygen. This is apparently insufficient, however, and it is possible that the reoxidized catalyst is of somewhat less active nature than the original. It should be noted that it is unlikely that oxygen removed from the catalyst can be replaced at low temperatures with the original binding energy.

The proposed model, reactions (E), (K), (F), (G), and

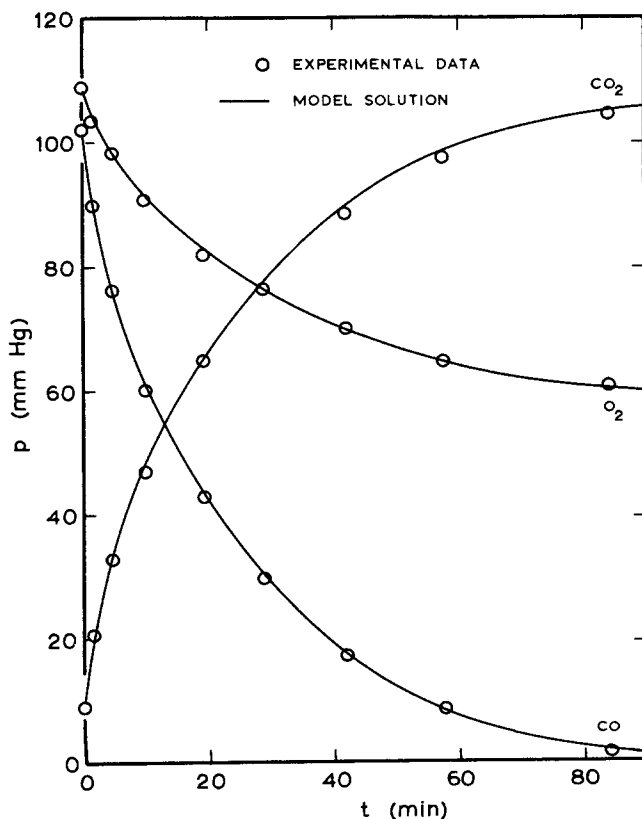


Fig. 7. Comparison of model with data, run B6.



(B), is based on a combination of gas-solid and classical catalytic processes and is somewhat similar to a model first proposed by Roginskii and Zeldovich (54, 57, 58, 74). The inclusion of  $O_s$  in the rate equation is consistent with earlier suggestions of a relationship between catalyst activity and available oxygen content (1, 9 to 12, 21, 38, 39, 43, 47, 52, 53, 61, 62, 65). Since  $O_s$  is variable, the rate of carbon monoxide adsorption as given by Equation (4) is not first-order in carbon monoxide, as has been suggested (1, 12, 14, 21, 23, 41, 61, 63, 65). Deviations from first-order kinetics are clearly apparent in the plotted results of other workers (14, 17, 45, 50, 62).

The behavior of the system was also suggestive of a nonuniformity in reactivity of the  $O_s$  sites other than that already considered in reactions (E) and (K). This has been reported or inferred in several places (12, 14, 26, 31, 34, 65) and is suggested in the use of the Elovich equation in connection with carbon monoxide adsorption (13, 21, 23, 45, 49, 54, 57, 58, 74) and its catalytic oxidation (5, 6, 17, 21, 23, 50, 55, 56). Incorporation of an Elovich type of characterization of surface heterogeneity into the model was considered unwarranted in view of the need for introduction of more parameters into a model already stretching the data.

The difficulties experienced in reproducibility of catalyst activities make determination of the true and isolated effect of temperature almost impossible. Thus, no estimates of activation energy are reported.

## CONCLUSIONS

The recirculation differential reactor proved well suited to the study of this reaction, particularly when used in conjunction with careful chromatographic analyses of the gas phase. The experimental system was generally successful with regard to our original aims of securing isothermal rate data at known partial pressures of the components (without assuming stoichiometric behavior) with a catalyst of reasonably well defined state. Water poisoning of the catalyst was eliminated, and diffusional effects were minimized.

Conversion-time data, when plotted in the common first-order form, exhibited important departures from first-order behavior. In early stages the reaction rate declines more rapidly than would a first-order reaction; later it declines less rapidly.

A mechanism to explain such behavior must be complex, and such is, indeed, the case. The essential character of it is the early predominance of reduction (and later oxidation) of the catalyst with carbon monoxide along with the reaction of adsorbed carbon monoxide with oxygen. The reduction and oxidation of the catalyst is proved by the gas analyses. The mechanism which incorporates many of the ideas in the literature is the most comprehensive yet proposed.

A kinetic model involving the five most important reactions of the mechanism is proposed, and rate constants for it evaluated. It is capable of closely reproducing the data, but it suffers from a considerable scatter among the constants. There is a variability in intrinsic catalyst activity not accounted for in this model. The success of the model cannot be considered as proof of the mechanism.

## ACKNOWLEDGMENT

The financial assistance of the National Science Foundation is gratefully acknowledged.

## NOTATION

$c_i$  = constants  
 $K$  = rate parameter, usually  $(\text{min.})^{-1}$

$k, k_i$  = absolute rate constants [usually  $(\text{min.})^{-1} (\text{mm. Hg.})^{-1}$ ]  
 $O_s$  = catalyst surface oxygen sites, equivalent mm. Hg.  
 $p$  = partial pressure, mm. Hg.  
 $S$  = vacant catalyst surface sites, equivalent mm. Hg.  
 $T$  = absolute temperature, °K.  
 $t$  = time, min.  
 $\theta$  = adsorbed carbon monoxide =  $O_s [\text{CO}]$

## Subscripts

$s$  = catalyst surface  
 $i$  = 1, 2, 3, . . .

## Superscript

0 = initial conditions at  $t = 0$

## LITERATURE CITED

1. Almquist, J. A., and N. C. Bray, *J. Am. Chem. Soc.*, **45**, 2305 (1923).
2. Bankloh, W., B. Chatterjee, and P. P. Das, *Trans. Indian Inst. Metals*, **4**, 271 (1950); *Chem. Abstr.*, **46**, 7415 (1952).
3. Barrett, E. P., L. G. Joyner, and P. P. Halenda, *J. Am. Chem. Soc.*, **73**, 373 (1951).
4. Benton, A. F., *ibid.*, **45**, 900 (1923).
5. Bielanski, A., in "Catalysis and Chemical Kinetics," p. 118, Academic Press, New York (1964).
6. ———, J. Deren, J. Haber, and J. Sloczynski, *Z. Physik. Chem. (N.F.)*, **24**, 345 (1960).
7. Brittan, M. I., Ph.D. dissertation, Yale Univ., New Haven, Conn. (1967).
8. Blyholder, G., *Proc. Intern. Congr. Catalysis*, 3rd, Amsterdam, **1**, 657, North-Holland, Amsterdam (1965).
9. Bray, N. C., and G. J. Doss, *J. Am. Chem. Soc.*, **48**, 2060 (1926).
10. Brooks, C. S., *J. Catalysis*, **4**, 535 (1965).
11. Bruns, B. P., *Acta Physicochim. URSS*, **7**, 875 (1937).
12. ———, and N. A. Shurmovskaya, *Zhur. Fiz. Khim.*, **32**, 2137 (1958).
13. Charachorin, F., and S. Yu. Elovich, *Acta Physicochim. URSS*, **5**, 325 (1936).
14. ———, S. Yu. Elovich and S. Z. Roginskii, *ibid.*, **3**, 503 (1935).
15. Christian, J. G., and J. E. Johnson, *Ind. Eng. Chem. Prod. Res. Develop.*, **2**, 235 (1963).
16. Chufarov, G. I., and M. F. Antonova, *Classe sci. tech.*, **381**, (1947); *Chem. Abstr.*, **42**, 3648 (1948).
17. Coue, J., P. C. Gravelle, R. E. Ranc, P. Rue, and S. J. Teichner, *Proc. Intern. Congr. Catalysis*, 3rd, Amsterdam, **1**, 748, North-Holland, Amsterdam (1965).
18. Dell, R. M., and F. S. Stone, *Trans. Faraday Soc.*, **50**, 501 (1954).
19. Dolique, R., and J. Galindo, *Bull. Soc. Chim. France, Memoires*, **10**, 64 (1943).
20. Eischens, R. P., and W. A. Pliskin, *Adv. Catalysis*, **9**, 662 (1957).
21. Elovich, S. Yu., and L. A. Kachur, *Zhur. Obshchei Khim.*, **9**, 714 (1939).
22. ———, and V. A. Korndorf, *ibid.*, **9**, 673 (1939).
23. ———, and S. Z. Roginskii, *Acta Physicochim. URSS*, **7**, 295 (1937).
24. Engelder, C. J., and M. Blumer, *J. Phys. Chem.*, **36**, 1353 (1932).
25. ———, and L. E. Miller, *ibid.*, **36**, 1345 (1932).
26. Foote, H. W., and J. K. Dixon, *J. Am. Chem. Soc.*, **53**, 55 (1931).
27. Frazer, J. C. W., and C. E. Greider, *J. Pys. Chem.*, **29**, 1099 (1925).
28. Garner, W. E., *J. Chem. Soc.*, 1239 (1947).
29. ———, T. J. Gray, and F. S. Stone, *Disc. Faraday Soc.*, **8**, 246 (1950).
30. ———, and T. Ward, *J. Chem. Soc.*, 857 (1939).
31. Hoskins, W. M., and N. C. Bray, *J. Am. Chem. Soc.*, **48**, 1454 (1926).
32. Hughes, E. E., and J. M. Thomas, *Fuel*, **41**, 297 (1962).
33. Karpacheva, S. M., and A. M. Rozen, *Dokl. Akad. Nauk*

- SSSR, 68, 1097 (1949).
34. ———, and A. M. Rozen, *Zhur. Fiz. Khim.*, 27, 146 (1953).
  35. Kasatkina, L. A., and V. G. Amerikov, *Kinetics and Catalysis*, 7, 86 (1966).
  36. ——— and A. P. Zuev, *ibid.*, 6, 413 (1965).
  37. Klier, K., and K. Kuchynka, *J. Catalysis*, 6, 62 (1966).
  38. Kuentzel, W. E., *J. Am. Chem. Soc.*, 52, 437 (1930).
  39. *Ibid.*, 445 (1930).
  40. Lamb, A. B., N. C. Bray, and J. C. W. Frazer, *J. Ind. Eng. Chem.*, 12, 213 (1920).
  41. ———, C. C. Scalione, and G. Edgar, *J. Am. Chem. Soc.*, 44, 738 (1922).
  42. ———, and W. E. Vail, *ibid.*, 47, 123 (1925).
  43. Loane, C. M., *J. Phys. Chem.*, 37, 615 (1933).
  44. Long, L. J., D. Eng. thesis, Yale Univ., New Haven, Conn., in preparation.
  45. Marcellini, R. P., R. E. Ranc, and S. J. Teichner, "Actes Congr. Intern. Catalyse, 2e, Paris, 1960," Vol. I, p. 289, Editions Technip, Paris (1961).
  46. Mathieu-Levy, L. S., and M. M. Geloso, *Bull. Soc. Chim. France*, 53, 1039 (1933).
  47. Merrill, D. R., and C. C. Scalione, *J. Am. Chem. Soc.*, 43, 1982 (1921).
  48. Moore, T. E., M. Ellis, and P. W. Selwood, *ibid.*, 72, 856 (1950).
  49. Najbar, M., K. Kuchynka, and K. Klier, *Coll. Czech. Chem. Comm.*, 31, 959 (1966).
  50. Parravano, G., *J. Am. Chem. Soc.*, 75, 1448 (1953).
  51. *Ibid.*, 1452 (1953).
  52. Rienacker, G., and E. Scheve, *Z. Anorg. Allgem. Chem.*, 330, 18, 27, 34 (1964).
  53. Rogers, T. H., C. S. Piggot, W. H. Bahlke, and J. M. Jennings, *J. Am. Chem. Soc.*, 43, 1973 (1921).
  54. Roginskii, S. Z. *Acta Physicochim. URSS*, 9, 475 (1938).
  55. ———, and T. F. Tselinskaya, *Zhur. Fiz. Khim.*, 21, 919 (1947); *Chem. Abstr.*, 42, 2500 (1948).
  56. *Ibid.*, 22, 1360 (1948); *Chem. Abstr.*, 43, 2498 (1949).
  57. Roginskii, S. Z., and Ya. Zeldovich, *Acta Physicochim. URSS*, 1, 554 (1934).
  58. *Ibid.*, 595 (1934).
  59. Rousseau, J., M. V. Mathieu, and B. Imelik, *Bull. Soc. Chim. France*, No. 8, 2608 (1966).
  60. Russell, R. G., personal communication (1966).
  61. Schwab, G.-M., and G. Drikos, *Z. physik. Chem.*, A185, 405 (1940).
  62. Shurmovskaya, N. A., and B. P. Burns, *Zhur. Fiz. Khim.*, 9, 301 (1937).
  63. *Ibid.*, 14, 1183 (1940); 24, 1174 (1950); *Chem. Abstr.*, 49, 2165 (1955).
  64. Vainshtein, F. M., and G. Ya. Turovskii, *Dokl. Akad. Nauk SSSR*, 72, 297 (1950).
  65. Vasil'ev, V. N., S. Yu. Elovich, and L. Ya. Margolis, *Dokl. Akad. Nauk SSSR*, 101, 703 (1955).
  66. Ward, T., *J. Chem. Soc.*, 1244 (1947).
  67. Weiss, M. D., M. Ch. E. thesis, Polytechnic Inst. Brooklyn, New York (1952).
  68. Weisz, P. B., and J. S. Hicks, *Chem. Eng. Sci.*, 17, 265 (1962).
  69. Whitesell, W. A., Ph.D. thesis, Johns Hopkins Univ., Baltimore, Md. (1923).
  70. ———, and J. C. W. Frazer, *J. Am. Chem. Soc.*, 45, 2841 (1923).
  71. Williamson, A. T., *ibid.*, 54, 3159 (1932).
  72. Winter, E. R. S., *Advan. Catalysis*, 10, 218 (1958).
  73. Yoshida, F., D. Ramaswami, and O. A. Hougen, *AIChE J.*, 8, 5 (1962).
  74. Zeldovich, Ya., *Acta Physicochim. URSS*, 1, 449 (1934); *Zhur. Fiz. Khim.*, 6, 234 (1935).

Manuscript received May 9, 1968; revision received September 11, 1968; paper accepted September 11, 1968.

## COMMUNICATIONS TO THE EDITOR

### A Bubble Growth Experiment for the Determination of Dynamic Surface Tension

CHARLES KIPPENHAN and DAVID TEGELER

University of Washington, Seattle, Washington

A number of techniques have been used for the measurement of dynamic surface tension of water-surfactant solutions (1 to 3). One very simple method, utilizing the phenomena of gas bubble formation on a submerged orifice, has been reported (4) but is difficult to apply because of a complicated analytical model. The process of gas bubbling from a submerged orifice into a pure liquid has been subdivided into three regions, namely, the constant volume (or single bubble) region, a transition zone, and a constant frequency region. The latter two taken together have also been referred to as the *regime of chain bubbling* (5 to 7). This note is based on observations made in the single bub-

ble region.

#### THE EXPERIMENT

The air bubbles were produced on an orifice which was submerged in a transparent plastic walled tank filled with either distilled water or water-surfactant solution. The particular solution used in this study was distilled water plus 0.08 vol. % of Ultra Wet 60L (Atlantic Refining Company, Los Angeles, California) which exhibited an equilibrium surface tension of 33 dynes/cm. as determined by the DeNouy Tensiometer method (maximum